ORIGINAL COMMUNICATION

Macro- and micro-structural insights into primary dystonia: a UK Biobank study

Claire L. MacIver[1,2] · Grace Bailey[1] · Pedro Luque Laguna[2] · Megan E. Wadon[2] · Ann-Kathrin Schalkamp[3] · Cynthia Sandor[3] · Derek K. Jones[2] · Chantal M. W. Tax[2,4] · Kathryn J. Peall[1]

Abstract

Background Dystonia is a hyperkinetic movement disorder with key motor network dysfunction implicated in pathophysiology. The UK Biobank encompasses > 500,000 participants, of whom 42,565 underwent brain MRI scanning. This study applied an optimized pre-processing pipeline, aimed at better accounting for artifact and improving data reliability, to assess for grey and white matter structural MRI changes between individuals diagnosed with primary dystonia and an unaffected control cohort.

Methods Individuals with dystonia ($n = 76$) were identified from the UK Biobank using published algorithms, alongside an age- and sex-matched unaffected control cohort ($n = 311$). Grey matter morphometric and diffusion measures were assessed, together with white matter diffusion tensor and diffusion kurtosis metrics using tractography and tractometry. Post-hoc Neurite Orientation and Density Distribution Imaging (NODDI) was also undertaken for tracts in which significant differences were observed.

Results Grey matter tremor-specific striatal differences were observed, with higher radial kurtosis. Tractography identified no white matter differences, however segmental tractometry identified localised differences, particularly in the superior cerebellar peduncles and anterior thalamic radiations, including higher fractional anisotropy and lower orientation distribution index in dystonia, compared to controls. Additional tremor-specific changes included lower neurite density index in the anterior thalamic radiations.

Conclusions Analysis of imaging data from one of the largest dystonia cohorts to date demonstrates microstructural differences in cerebellar and thalamic white matter connections, with architectural differences such as less orientation dispersion potentially being a component of the morphological structural changes implicated in dystonia. Distinct tremor-related imaging features are also implicated in both grey and white matter.

Keywords Dystonia · MRI · Diffusion MRI · Structural MRI

Chantal M. W. Tax and Kathryn J. Peall are contributed equally to this work.

✉ Claire L. MacIver
maciverc@cardiff.ac.uk

1 Division of Psychological Medicine and Clinical Neurosciences, Neuroscience and Mental Health Research Institute, Cardiff University School of Medicine, Cardiff, UK

2 Cardiff University Brain Imaging Centre (CUBRIC), Cardiff University, Cardiff, UK

3 Division of Psychological Medicine and Clinical Neurosciences, UK Dementia Research Institute, Cardiff University, Cardiff, UK

4 Image Sciences Institute, University Medical Center Utrecht, Utrecht, The Netherlands

Introduction

Dystonia is a hyperkinetic movement disorder involving involuntary, repetitive or sustained muscle contractions, estimated to affect up to 120/100,000 population [4]. Dystonia may arise as a primary disorder, or part of a wider neurodevelopmental or neurodegenerative condition, with both genetic and idiopathic forms, and a spectrum of motor distributions. Although the pathophysiological mechanisms of dystonia remain uncertain, animal models implicate disrupted striatal GABA transmission [15] and cerebellar Purkinje cell ectopic dendritic spines [21], while stem cell models have noted functional hyperexcitability, changes to dendritic branching patterns and abnormalities in synaptic

plasticity and cellular stress response pathways [29, 32]. Other neurotransmitter systems have additionally been implicated, particularly within the striatal structures, with decreased and irregular cholinergic interneuron firing and reduced inhibitory effect of dopamine receptor agonists [26, 43].

Human neuroimaging has demonstrated reduced network-based functional connectivity between the basal ganglia, sensorimotor and frontoparietal regions [6], alongside disruption to neuronal inhibitory/excitatory balance, with reduced GABA binding and lower post-movement event-related synchronisation of beta activity [14, 33]. Volumetric MRI has indicated higher volumes in task-specific forms of dystonia, most notably in the cerebellar, basal ganglia and sensorimotor grey matter regions [34], with variable findings in non-task-specific forms. Findings from diffusion MRI (dMRI) studies have been mixed, although cerebellar white matter projections, and white matter deep to the primary sensorimotor cortices have been highlighted [23]. There is also evidence for genotypic and phenotypic variation, including more widespread changes in genetic dystonias and intermediate changes in non-motor manifesting gene carriers. In addition, most existing literature uses non-specific analysis strategies such as fractional anisotropy (FA) [23] averaged along a neuronal tract, with these providing limited biological insight into the pathological underpinnings.

The UK Biobank (http://www.ukbiobank.ac.uk) is a prospective database containing health-related data for > 500,000 participants across the UK, with previous work identifying 1572 individuals diagnosed with dystonia within this cohort [38]. Brain MRI was undertaken in a subset of the overall cohort ($n = 42,565$) including T1-weighted and multi-shell diffusion weighted sequences [8]. Here, we aim to assess whether diffusion based microstructural MRI parameters differ in key motor grey matter, notably cerebellar, basal ganglia, thalamic and sensorimotor grey matter, and their interconnecting white matters pathways, in the dystonia cohort in the UK Biobank compared to age- and sex-matched unaffected controls. Additionally, and in light of the suggestion from previous studies that imaging changes may differ across distinct dystonia subtypes [7], we have also analyzed the largest individual diagnostic groups—cervical dystonia and dystonic tremor—again, with comparison to the control cohort (Fig. 1).

Methods

Cohort derivation and characteristics

Identification of the UK Biobank dystonia cohort used a clinically validated algorithm derived from a national clinically linked databank [4, 38]. This made use of ICD-10 codes derived from NHS hospital records (UK Biobank data fields 41,202, 41,204 and 41,207) and Primary care records (Read codes v2, data portal field read_2), with inclusion and exclusion diagnoses outlined in Supplementary Table 1. All individuals identified as having been diagnosed with dystonia and who had undergone T_1-weighted and diffusion-weighted brain MRI were included (UK Biobank application number 69610). A 1:4 age- and sex-matched control cohort was derived from the overall cohort following application of the same exclusion criteria as was used for identification of the dystonia cohort [38]. Scans marked by the UKBB as 'unusable' (based on pathology or T1 artifact) were visually inspected and only excluded if pathology was identifiable. Participants were excluded from the diffusion-based analyses if they had missing or incomplete diffusion-weighted imaging data or were marked by the UKBB as 'incompatible' due to use of a different acquisition protocol.

Imaging acquisition

Imaging was undertaken in one of four centres (Table 1) using a 3 T Siemens Skyra scanner with a standard Siemens 32-channel radiofrequency receive head coil, using a standardised acquisition protocol across sites. A sagittal 3D T_1-weighted MPRAGE was acquired, with field of view $208 \times 256 \times 256$ and voxel size 1mmx1mmx1mm. The dMRI acquisition used a spin echo planar imaging sequence with $\times 3$ multi-slice acceleration, fat saturation, field of view $104 \times 104 \times 72$, and voxel dimensions 2mm $\times$ 2mm $\times$ 2mm. Fifty distinct diffusion directions were acquired each for $b = 1000$ s/mm^2 and $b = 2000$s/mm^2, with 5 $b = 0$ s/mm^2 images. A 6/8 partial Fourier readout was used [1, 24].

dMRI preprocessing and parameter estimation

dMRI data are processed within the UK Biobank using standardised pipelines. However, significant variability of approach exists in diffusion imaging analysis, and while there is no current evidence based consensus on optimal approaches, attempts have been made to optimize methodology to reduce the impact of imaging artefacts on dMRI data [2]. For this study, a local, optimized preprocessing pipeline was applied to the raw diffusion data (with facial feature removal prior to UK Biobank data release), described in Fig. 1A. This involved brain extraction, denoising [35], outlier detection (e.g., due to signal dropout from motion) [31], signal drift correction, and correction for Gibbs ringing [18], eddy currents, susceptibility distortion and subject motion [3], and gradient non linearities [5]. Each of the analytical steps were manually reviewed for a randomly selected 10% subset to assess data quality. Parameter estimation used a diffusion kurtosis representation and a constrained weighted least squares fitting approach with weight reduction for outlier measurement [30, 37], demonstrated to

Fig. 1 Schematic of methodology. **a** outline of analysis methodology; **b** grey matter regions of interest; **c** white matter tracts assessed with tractography; those shown in bold are used in the tractometry analysis; **d** recruitment flowchart showing final inclusions and exclusions. *dMRI* diffusion magnetic resonance imaging; *DKI* diffusion kurtosis imaging; *ROI* region of interest; *FA* fractional anisotropy; *MD* mean diffusivity; *MK* mean kurtosis; *AK* axial kurtosis; *RK* radial kurtosis
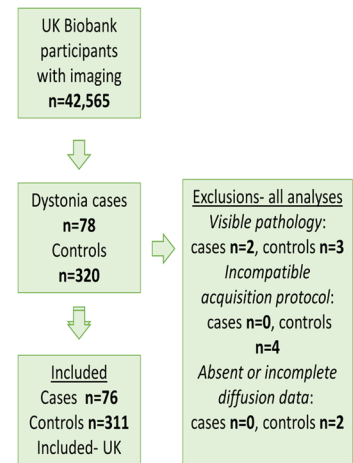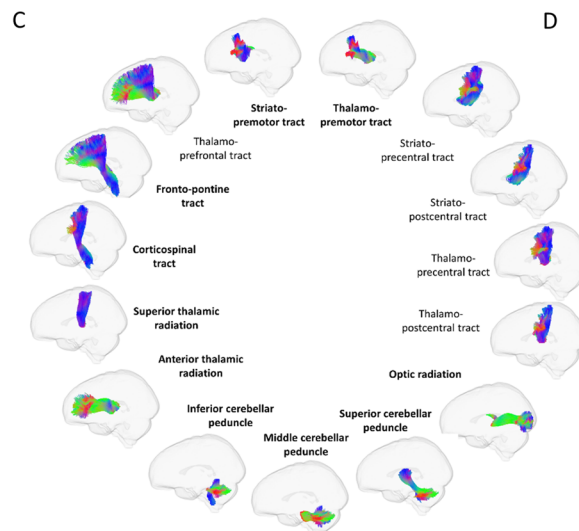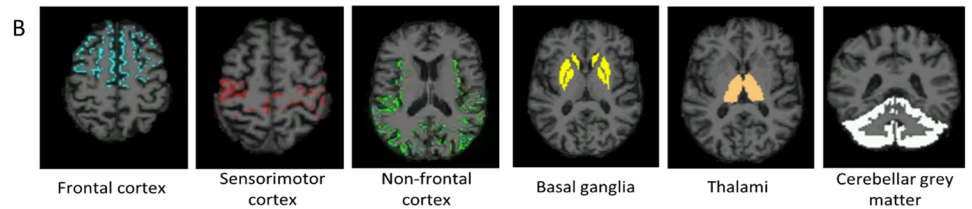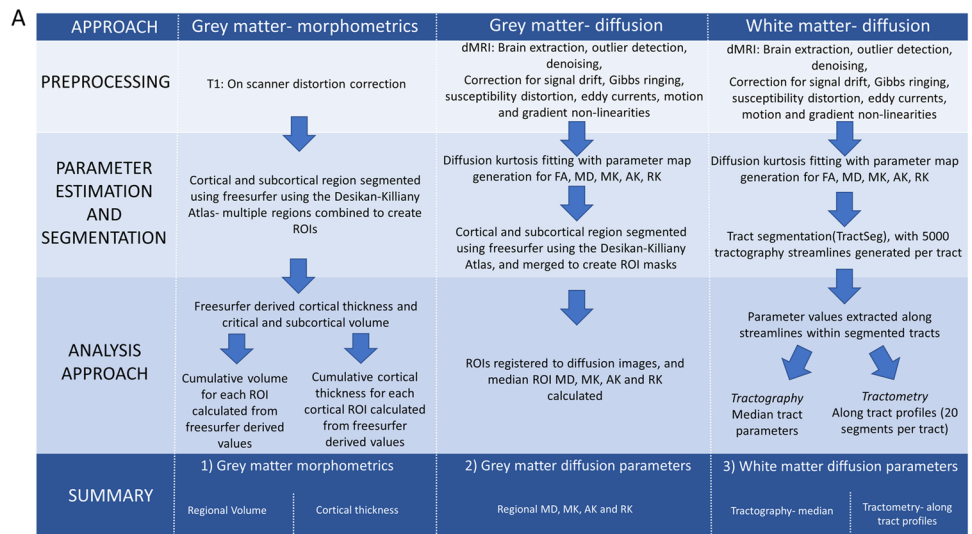
enable more accurate estimation of diffusion tensor imaging (DTI) parameters [36] than more standard DTI fitting approaches. Parameter maps were created for FA, mean diffusivity (MD), mean kurtosis (MK), axial kurtosis (AK) and radial kurtosis (RK). These parameter maps were additionally used in the grey matter analysis detailed below.

Analysis approach

Grey matter analysis

The raw T_1-weighted images were used for grey matter

Table 1 Participant demographics and dystonia subgroups

Group	Number of cases	Male: Female (n)	Median Age-years (s.d.)	Number of individuals scanned at individual MRI locations (Cheadle/Reading/Newcastle/Bristol)
Unaffected control cohort	311	132:179	64.62 (8.93)	40/22/14/0
Whole dystonia cohort	76	31:45	64.16 (8.75)	180/44/86/1
Idiopathic torsion dystonia	0	–	–	–
Idiopathic non-familial dystonia	0	–	–	–
Idiopathic familial dystonia	0	–	–	–
Cervical dystonia	40	17:23	62.68 (8.87)	23/9/8/0
Idiopathic orofacial dystonia	2	2:0	58 (11.31)	0/2/0/0
Blepharospasm	9	3:6	72 (7.98)	4/2/1/0
Writer's cramp	0	–	–	–
Myoclonic dystonia	0	–	–	–
Segawa syndrome	0	–	–	–
Unspecified tremor	17	10:7	68.53 (8.33)	7/7/3/0
Unspecified dystonia	10	0:10	61 (6.52)	6/2/2/0

segmentation using Freesurfer [13], with six region of interest (ROI) masks created from these segmentations (prefrontal, sensorimotor, non-frontal, striatal, thalamic and cerebellar cortical masks, Fig. 1A & B, Supplementary Table 2). Within each ROI, total cortical thickness (summed subregion values) and total volume were calculated, with the latter also calculated for subcortical regions. Grey matter diffusion measures were calculated with the first $b = 0$ image registered to the brain extracted T_1-weighted image for each participant (using FSL EPI reg [17]), and the inverse of this transform applied to the GM ROIs with nearest neighbour interpolation into diffusion space. Voxels with partial volume with other tissues due to the differing voxel dimensions were excluded and median ROI MD, MK, AK and RK were calculated (from the diffusion kurtosis parameter maps).

White matter analysis

Within the white matter pathways, we evaluated both whole tract averages (tractography) and along-tract profiling (tractometry), investigating evidence of localised changes in tract morphology, as has been shown in genetically homogenous dystonia cohorts [9]. Tractseg [40] was used to segment the motor tracts: middle cerebellar peduncle, bilateral inferior cerebellar peduncles, superior cerebellar peduncles, frontopontine tracts, corticospinal tracts, anterior thalamic radiations, superior thalamic radiations, thalamoprefrontal tracts, thalamopremotor tracts, thalamoprecentral tracts, thalamopostcentral tracts, striatopremotor, striatoprecentral tracts and striatopostcentral tracts (Fig. 1C). Optic radiations were included as a non-motor comparison tract [23]. Multi-shell multi-tissue constrained spherical deconvolution was applied to the preprocessed diffusion images to extract the white

matter fODF, with subsequent peak-extraction limited to a maximum of three peaks/voxel. A fully-connected convolutional neural network was used to create a tract probability image for each orientation and tract, with start and end regions segmented and fibre orientation maps calculated within the segmented regions [42]. Probabilistic tractography [41] with 5000 streamlines was performed within each segmented region, with median parameter diffusion tensor values (FA and MD) and diffusion kurtosis values (MK, AK and RK) extracted from the streamlines. In addition, along-tract profiling (tractometry) was performed [11, 39]: the tracts were portioned into 20 segments along their length with the centroid of all streamlines within each segment identified, the end two segments excluded and median value across streamlines calculated for each of the 18 remaining segments [11]. The thalamoprefrontal, thalamoprecentral, striatoprecentral, thalamopostcentral and striatopostcentral tracts were excluded from tractometry analysis due to their geometry not enabling consistent segmentations to be produced.

Neurite orientation and dispersion density index (NODDI)

Tracts where significant differences were observed between the dystonia and control cohorts were further examined using white matter compartmental parameters (OD—orientation dispersion index, ND—neurite density index, and FWF—free water signal fraction), estimated using post-hoc Neurite Orientation, Dispersion and Density Imaging (NODDI) [44], hypothesized to better disentangle biological features. This was performed for tracts that demonstrated significant differences in any of the original analyses. As the tractometry

analyses demonstrated visually corresponding tract profiles for left and right tracts, the two were combined for this post hoc analysis.

Statistical analysis

Analysis was undertaken using RStudio v0.99.892. Participant demographic information was summarised using descriptive statistics. Simple linear regression models were applied comparing disease status (independent variable) for each parameter and tract (dependent variables). Subgroup analyses were performed for the two largest diagnostic subgroups—cervical dystonia and dystonic tremor—compared to unaffected controls. Bonferroni correction for multiple comparisons was applied for both tracts and parameters, with differences reported only if p-values were significant ($p < 0.05$) following correction.

Results

Demographics

Initially, 78 individuals diagnosed with dystonia and 320 control participants with imaging data were identified. Of these, two dystonia and 9 control cases were excluded due to visible pathology (cases $n = 2$ (extensive white matter changes $n = 1$, hydrocephalus $n = 1$), controls $n = 3$ (extensive white matter changes $n = 2$, congenital malformation $n = 1$)), incompatible acquisition protocols ($n = 4$) or absent/incomplete diffusion data ($n = 2$), Therefore, a total of 76 individuals with dystonia and 311 healthy controls were included for onward analysis. Median age at scanning for both patient and control groups was 64 (SD 8.87 and 8.91 respectively), with a male to female ratio of 1:1.44 for both groups. Dystonia cases were subdivided based on available clinical diagnoses, with the two largest groups being cervical dystonia ($n = 40$) and dystonic tremor ($n = 17$) (Table 1).

Grey matter analysis

No significant differences in regional volume or cortical thickness were observed when comparing the overall dystonia, cervical or tremor cohorts to unaffected controls. Diffusion kurtosis measures showed significant differences only in the striatum for the tremor cohort, with a higher RK values ($p = 5.84 \times 10^{-4}$) compared to controls (Fig. 2).

White matter analysis

Tractography

No significant diffusion tensor (FA or MD) or diffusion kurtosis (MK, AK, RK) differences were observed between the overall cohort, cervical or dystonic tremor cohorts, compared to the unaffected control group (Supplementary Fig. 1).

Tractometry

For tracts in which significant differences were observed, along-tract profiles are included in Figs. 3, 4, 5 (Supplementary Figs. 2, 3, 4 display all tract analyses).

Overall dystonia cohort vs. unaffected control group

Figure 3 demonstrates higher FA in the mid right superior cerebellar peduncle ($p = 2.69 \times 10^{-4}$), while NODDI identified significant changes to ODI measures across the same tract (lower mid-tract ($p = 7.19 \times 10^{-4}$) and higher distal tract ($p = 3.3 \times 10^{-7}$), as well as significantly lower NDI ($p = 6.8 \times 10^{-4}$) and FWF ($p = 0.002$) values in the dystonia cohort. ODI differences were also demonstrated in the anterior thalamic radiations (higher proximal-mid ($p = 6.53 \times 10^{-5}$) and distal ($p = 1.96 \times 10^{-4}$) values) and striatopremotor (lower mid-tract values ($p = 0.001$) tracts in the dystonia cohort.

Cervical dystonia cohort vs. unaffected control group

No significant differences were observed for DTI and DKI measures (Fig. 4). NODDI identified differences in ODI in the superior cerebellar peduncles (higher proximal ($p = 0.002$) and lower mid ($p = 4.17 \times 10^{-4}$) and distal ($p = 1.2 \times 10^{-4}$) values), and anterior thalamic radiations (lower distal values ($p = 7.37 \times 10^{-4}$)) in the cervical dystonia cohort compared to controls Fig. 5.

Dystonia with tremor vs. unaffected control group

Multiple regions of significant difference were observed across the superior cerebellar peduncle and anterior thalamic radiation, including FA (right, higher in tremor ($p = 5.22 \times 10^{-4}$)), MD (left, higher in tremor ($p = 3.43 \times 10^{-4}$)), MK (left, lower in tremor ($p = 4.59 \times 10^{-4}$)) and AK (left, lower in tremor ($p = 1.92 \times 10^{-4}$)) in the anterior thalamic radiations, with higher FA ($p = 6.61 \times 10^{-5}$) found in the right superior cerebellar peduncle. These were coupled with corresponding changes in NODDI measures, with lower ODI ($p = 4.31 \times 10^{-4}$) and higher NDI ($p = 8.44 \times 10^{-5}$) in the superior cerebellar peduncles, and lower ODI ($p = 8.3 \times 10^{-5}$) and lower NDI ($p = 5.96 \times 10^{-4}$) in the anterior thalamic radiations. Differences were additionally observed in the right striatopremotor tract (right tract, higher FA ($p = 4.71 \times 10^{-4}$)) and optic radiations (left tract, higher FA ($p = 1.78 \times 10^{-7}$), and higher distal FWF

Fig. 2 Box plots showing median values for dystonia and controls. **a** regional volume; **b** cortical thickness; **c** Diffusion measures. Significant differences on linear model following multiple comparison correction are highlighted with *
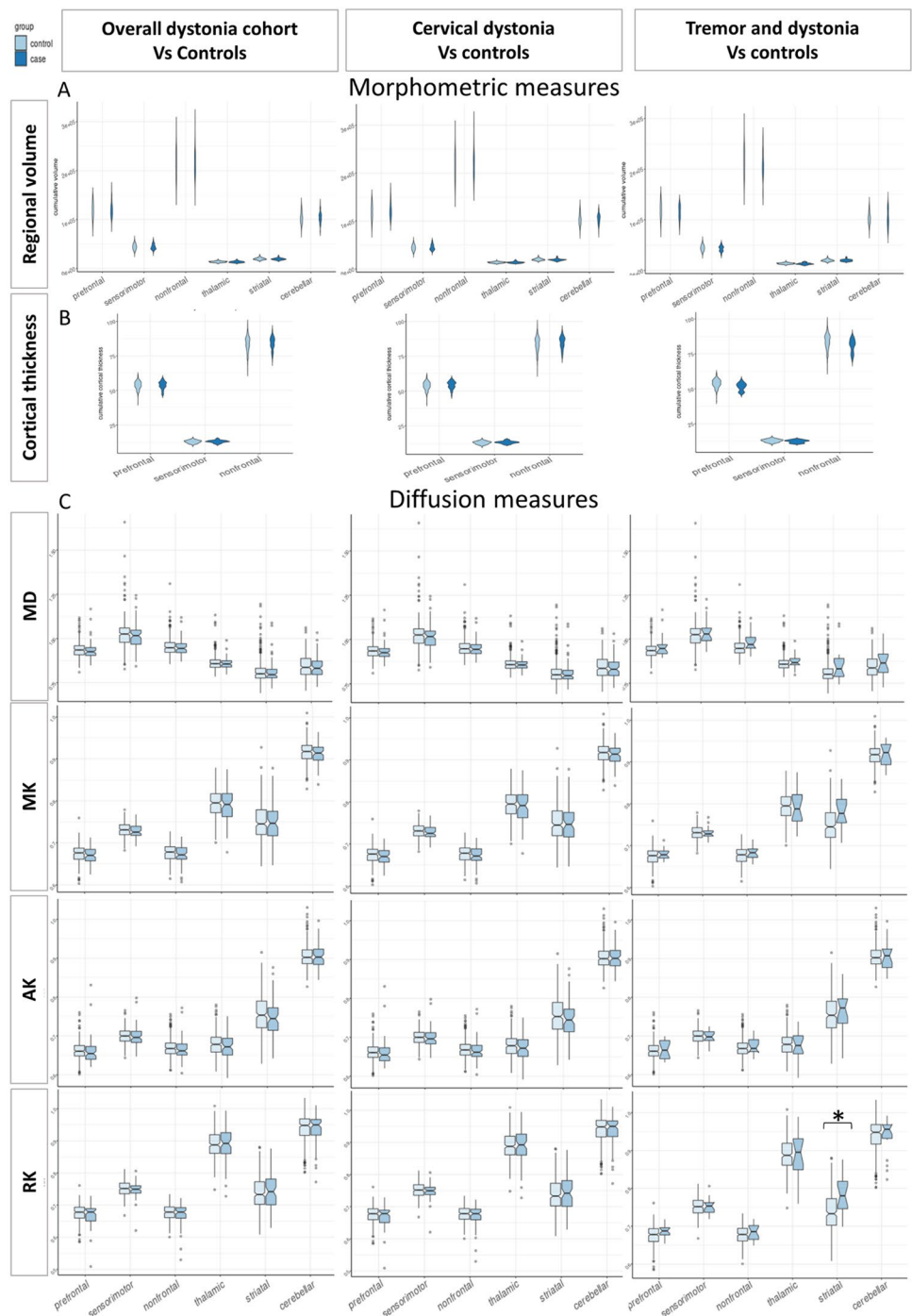

$(p = 1.6 \times 10^{-7}))$ in the dystonic tremor group compared to controls.

Discussion

This study analyses T1- and diffusion-weighted brain MRI in a large dystonia cohort, identified from the UK Biobank cohort, using an optimized imaging processing approach. It provides evidence of both grey and white matter microstructural differences in key motor networks in dystonia, with striatal grey matter kurtosis differences, and localised white matter differences in key motor tracts, notably the superior cerebellar peduncle, anterior thalamic radiations and striatopremotor tracts (Fig. 6).
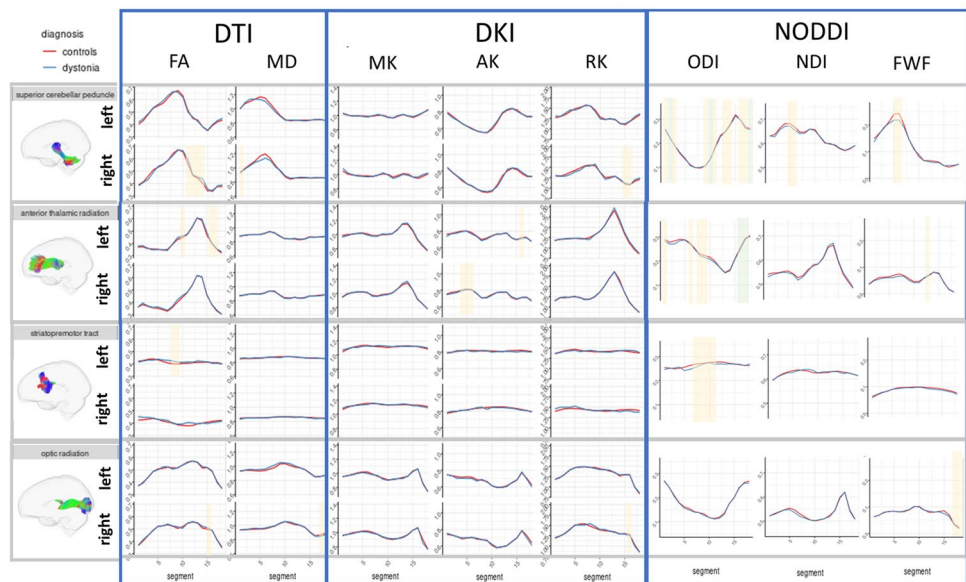
Tractometry findings: Whole cohort compared to controls
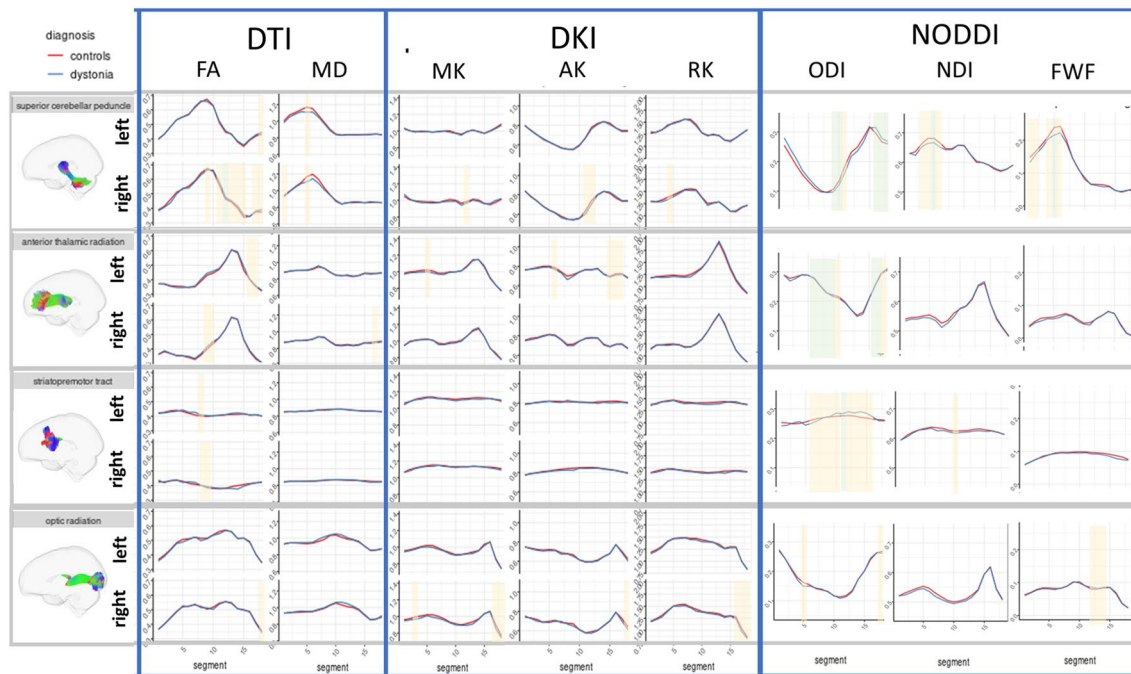
Fig. 3 Along tract profiles (tractometry) for the whole dystonia cohort compared to controls. Green shaded regions represent statistically significant linear model results following multiple comparison correction. Yellow shaded regions are significant ($p < 0.050$) prior to correction

Fig. 4 Along tract profiles (tractometry) for the cervical dystonia cohort compared to controls. Green shaded regions represent statistically significant linear model results following multiple comparison correction. Yellow shaded regions are significant ($p < 0.050$) prior to correction

Tractometry findings: Cervical Dystonia compared to controls
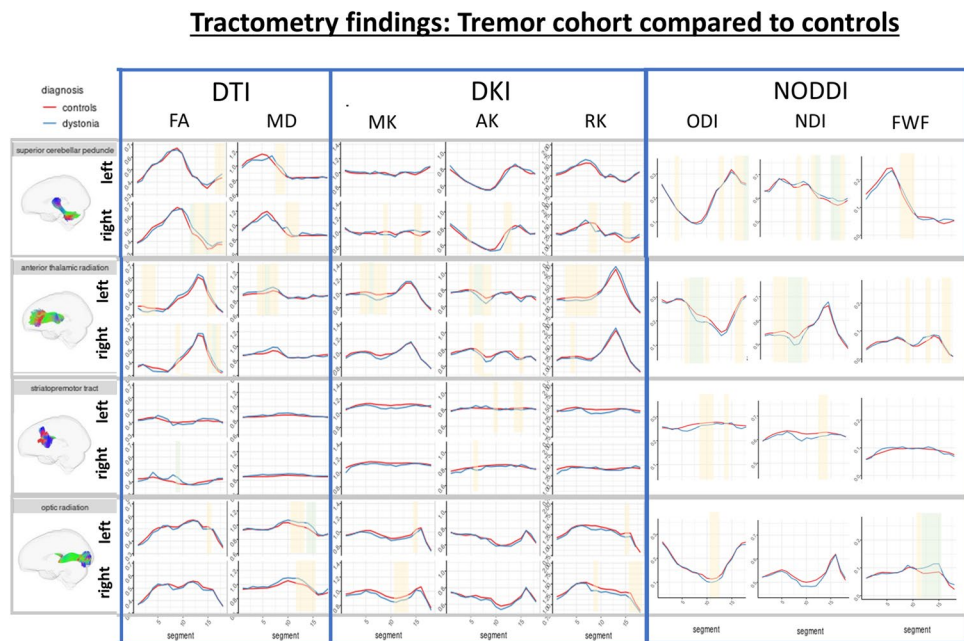

Grey matter

Morphometric analyses demonstrated no between group differences for the overall or subgroup analyses. This is partially at odds with existing literature, particularly in genetic and task specific forms of dystonia [16, 27]. However, non-task-specific dystonias, such as cervical dystonia and blepharospasm, have demonstrated substantial variability in both the presence and direction of any identified volumetric differences. Minimal existing work has investigated GM in

Fig. 5 Along tract profiles (tractometry) for the tremor cohort compared to controls. Green shaded regions represent statistically significant linear model results following multiple comparison correction. Yellow shaded regions are significant (*p* < 0.050) prior to correction

Tractometry findings: Tremor cohort compared to controls

dystonic tremor, identifying increases in the inferior frontal cortex [19], motor cortex [10] and striatal [19] volumes/thickness. Not previously applied in a dystonia cohort, grey matter diffusion kurtosis measures here identified tremor-specific striatal differences, with significantly higher RK values. Previous work has shown diffusion kurtosis measures to be correlated with brain microstructural changes, including during normal brain development [25] and in white matter in multiple sclerosis [22]. The differences observed may indicate subtle morphological striatal changes, particular to tremor, such as in cell body density or dendritic branching complexity, however, the MR acquisition methodology used as part of the UK Biobank study is insufficient to apply modelling approaches to ascertain the nature of this signal difference. Approaches which provide additional information on tissue heterogeneity, including compartmentalisation into neurites and soma, may facilitate better understanding and insight into these observed differences.
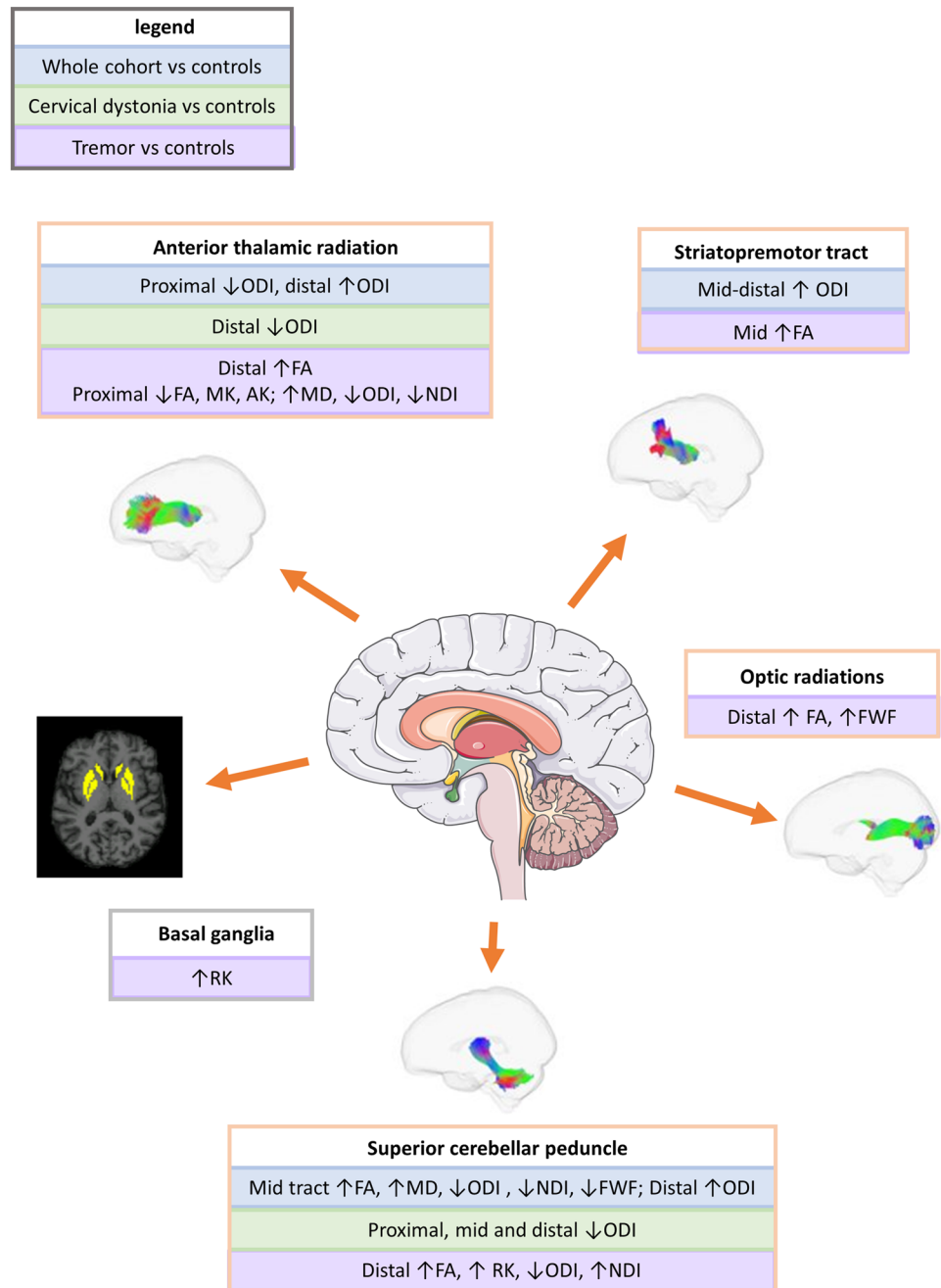
White matter

Tractography identified no significant differences between groups, although multiple tracts had significantly higher FA values in the dystonia cohort compared to controls prior to correction for multiple comparisons. Tractometry, aimed at identifying regional variation along individual tracts, identified localized differences, most notably higher FA in the superior cerebellar peduncles, anterior thalamic radiations and striatopremotor tracts (Fig. 6). These higher FA values are potentially explained by disrupted inhibition resulting in increased pathway activation and subsequent increased muscle activity, or conversely could reflect a mechanism

of attempted compensation for muscle overactivation. While studies involving cohorts of individuals diagnosed with genetic dystonias have often identified lower (rather than higher) FA values, those involving idiopathic forms (comprising the majority of this cohort) have reported more mixed results with some identifying lower MD or higher FA in corroboration with our findings, while only a few have found lower FA values [7, 12, 28]. The dissonance may reflect the heterogeneity of different dystonia diagnoses with varying underlying pathological processes, including, for example, disruption to white matter tract integrity in some forms, with others such as adult onset idiopathic dystonias involving differing mechanism such as reinforcement of selected projections. Alternatively, aberrance of earlier life neurodevelopmental processes may be involved, such as the pruning of dendritic connections and increases in the complexity of WM pathway course, which later decompensate and clinically manifest as a focal dystonia. The optic radiations, included as a non-motor comparison, unexpectedly demonstrated distally higher FA in the tremor cohort, with a few studies previously implicating visual regions in dystonia [28]. This may reflect compensatory visual system processes given the role of visual feedback in movement, or evidence of more diffuse microstructural changes within the brain.

Post hoc NODDI was undertaken as it is hypothesized to provide more microstructurally meaningful interpretation of signal differences, demonstrating more pronounced localised differences in the tracts implicated in DTI and DKI analysis. The superior cerebellar peduncles and thalamic radiations were the most dominantly implicated, with ODI the measure in which greatest variation between groups was observed, with overall lower values in the dystonia cohort. This

Fig. 6 Summary of key findings. *FA* fractional anisotropy; *MD* mean diffusivity; *MK* mean kurtosis; *AK* axial kurtosis; *RK* radial kurtosis; *ODI* orientation distribution index; *NDI* neurite density index

legend
Whole cohort vs controls
Cervical dystonia vs controls
Tremor vs controls

Anterior thalamic radiation
Proximal ↓ODI, distal ↑ODI
Distal ↓ODI
Distal ↑FA
Proximal ↓FA, MK, AK; ↑MD, ↓ODI, ↓NDI

Striatopremotor tract
Mid-distal ↑ ODI
Mid ↑FA

Optic radiations
Distal ↑ FA, ↑FWF

Basal ganglia
↑RK

Superior cerebellar peduncle
Mid tract ↑FA, ↑MD, ↓ODI , ↓NDI, ↓FWF; Distal ↑ODI
Proximal, mid and distal ↓ODI
Distal ↑FA, ↑ RK, ↓ODI, ↑NDI

corresponds with the FA differences outlined above, and the suggestion of 'over-use' of subsets of neuronal pathways in giving rise to dystonia. Further interpretation of the ODI NODDI measure could suggest that white matter changes in idiopathic dystonia are related to disruption to the organisation and dispersion of fibres within tracts, rather than differences in axonal morphology. However,—in the superior cerebellar peduncles for the overall dystonia cohort, and for the superior cerebellar peduncles, anterior thalamic radiations and the optic radiations for the tremor cohort compared to controls—differences in NDI and FWF measures were also

observed, potentially indicating a degree of morphological change to the axons themselves in these regions, which may reflect secondary adaptation or an alternative primary pathological process. No previous work has applied NODDI in a dystonia cohort for comparison, although one fixel-based analysis approach has identified a lower Fibre Density value in the striatal region [45].

Differences, compared to the control cohort, were most frequently observed in the tremor cohort, observed across both grey and white matter measures. Several more recent studies have indicated that distinct imaging changes are

observed when both tremor and focal dystonia are observed, compared to isolated, focal dystonia alone. Suggested explanations for this include adaptive changes, particular to tremor, rather than of the dystonic syndrome itself. The limited dystonia subgroup sizes and phenotypic detail available within the UK Biobank dataset doesn't allow for a direct tremor versus no tremor comparison, however, a previous comparison of dystonic and essential tremor identified higher FA in cerebellar projections, regardless of tremor type but to a greater extent within the dystonic tremor cohort, with wider evidence existing of differences between tremulous and non-tremulous dystonia forms [7]. One limitation of the limited phenotypic data available in the UK Biobank is the inability to determine body part affected by tremor, with this broad diagnostic category likely encompassing multiple phenotypic subgroups which may have differing imaging correlates. Additionally, whilst a diagnosis of essential tremor is applied as an exclusion criteria (Supplementary material 1), there is potential that a portion of this group would fall into this diagnostic category, and so the tremor group and resultant findings may represent a broader range of the tremor spectrum than dystonic tremor alone.

As we observed, whole tract average tractography approaches potentially overlook localized pathway changes, with along-tract profiling (tractometry) providing more anatomically specific localised assessment, undertaken here for the first time in dystonia. Despite this advantage, diffusion tensor and kurtosis measures remain non-specific even when profiled along a tract. Biophysical models such as NODDI aim to overcome some limitations of traditional DTI and DKI approaches by modelling tissue microstructural properties such as intra- and extra-axonal compartments. However, estimating microstructural parameters with acquisitions at low-to-moderate b-values (as used in this acquisition) is notoriously difficult due to inherent degeneracy (where multiple physically plausible parameter settings result in the same signal decay) and requires a priori fixing or linking of values, limiting the ability to capture true biophysical changes [20]. Hence, these measures should be interpreted with caution, and more extensive acquisitions are necessary to map more specific microstructural features. A further limitation of this dataset is the lack of in-depth clinical phenotyping data available, with the heterogeneous spectrum of dystonic disorders reduced to broad diagnostic categories providing minimal insight into the specific motor (or non-motor) phenotype of the participants. This limits potential interpretation of the findings seen here and requires further work in well phenotyped and homogenous cohorts in future to delineate syndrome and symptom specific differences. This is a particularly dominant factor within the overall cohort analysis, where potentially differences between the dystonia syndromes may have differing impacts, either cancelling or diluting the resultant imaging differences seen. To assess whether the cervical dystonia cases, comprising the majority of the overall cohort, were having excess impact on the overall analysis, we performed a Cohen's D effect size calculation between the cervical and non-cervical dystonia cases for two key regions, finding no meaningful between group differences (ODI measure in the mid anterior thalamic radiation: 0.029; FA in the mid-distal right superior cerebellar peduncle: 0.097). Additionally, whether the differences seen are causative or compensatory cannot be established via a cross-sectional imaging study, with longitudinal and animal model studies necessary to attempt to disentangle this point. Cross site image acquisition differences have additional potential to influence findings in a study such as this, however, previous work in UK Biobank data has demonstrated that this variation in image centre has had minimal impact on study findings [2].

Overall, this work demonstrates microstructural motor pathway differences in idiopathic forms of dystonia, with additional changes that appear to be specific to when dystonia and tremor are observed together. Further work is needed to develop and apply more biologically meaningful and specific in vivo human imaging measures, in robustly phenotyped clinical cohorts, that may better allow disentanglement of potential underlying brain morphological and microstructural differences and advance mechanistic understanding in dystonia.

Declarations

Conflicts of interest On behalf of all authors, the corresponding author states that there is no conflict of interest. The authors have no relevant

financial or non-financial interests to disclose. The authors have no competing interests to declare that are relevant to the content of this article.

Ethical standards The UK biobank study has been approved by the appropriate ethics committee and has therefore been performed in accordance with the ethical standards laid down in the 1964 Declaration of Helsinki and its later amendments. All persons gave their informed consent prior to their inclusion in the study.

Open Access This article is licensed under a Creative Commons Attribution 4.0 International License, which permits use, sharing, adaptation, distribution and reproduction in any medium or format, as long as you give appropriate credit to the original author(s) and the source, provide a link to the Creative Commons licence, and indicate if changes were made. The images or other third party material in this article are included in the article's Creative Commons licence, unless indicated otherwise in a credit line to the material. If material is not included in the article's Creative Commons licence and your intended use is not permitted by statutory regulation or exceeds the permitted use, you will need to obtain permission directly from the copyright holder. To view a copy of this licence, visit http://creativecommons.org/licenses/by/4.0/.

References

1. Alfaro-Almagro F, Jenkinson M, Bangerter NK, Andersson JLR, Griffanti L, Douaud G, Sotiropoulos SN, Jbabdi S, Hernandez-Fernandez M, Vallee E, Vidaurre D, Webster M, McCarthy P, Rorden C, Daducci A, Alexander DC, Zhang H, Dragonu I, Matthews PM, Miller KL, Smith SM (2018) Image processing and Quality Control for the first 10,000 brain imaging datasets from UK Biobank. Neuroimage 166:400–424

2. Alfaro-Almagro F, McCarthy P, Afyouni S, Anderson JLR, Bastiani M, Miller KL, Nichols TE, Smith SM (2020) Confound modelling in UK Biobank brain imaging. bioRxiv:2020.2003.2011.987693

3. Andersson JLR, Sotiropoulos SN (2016) An integrated approach to correction for off-resonance effects and subject movement in diffusion MR imaging. Neuroimage 125:1063–1078

4. Bailey GA, Rawlings A, Torabi F, Pickrell O, Peall KJ (2022) Adult-onset idiopathic dystonia: a national data-linkage study to determine epidemiological, social deprivation, and mortality characteristics. Eur J Neurol 29:91–104

5. Bammer R, Markl M, Barnett A, Acar B, Alley MT, Pelc NJ, Glover GH, Moseley ME (2003) Analysis and generalized correction of the effect of spatial gradient field distortions in diffusion-weighted imaging. Magn Reson Med 50:560–569

6. Battistella G, Simonyan K (2019) Top-down alteration of functional connectivity within the sensorimotor network in focal dystonia. Neurology 92:e1843–e1851

7. Bédard P, Panyakaew P, Cho HJ, Hallett M, Horovitz SG (2022) Multimodal imaging of essential tremor and dystonic tremor. NeuroImage Clinical 36:103247

8. Bycroft C, Freeman C, Petkova D, Band G, Elliott LT, Sharp K, Motyer A, Vukcevic D, Delaneau O, O'Connell J, Cortes A, Welsh S, Young A, Effingham M, McVean G, Leslie S, Allen N, Donnelly P, Marchini J (2018) The UK Biobank resource with deep phenotyping and genomic data. Nature 562:203–209

9. Carbon M, Kingsley PB, Tang C, Bressman S, Eidelberg D (2008) Microstructural white matter changes in primary torsion dystonia. Movem Disord 23:234–239

10. Cerasa A, Nistico R, Salsone M, Bono F, Salvino D, Morelli M, Arabia G, Quattrone A (2014) Neuroanatomical correlates of dystonic tremor: a cross-sectional study. Parkinsonism Relat Disord 20:314–317

11. Chandio BQ, Risacher SL, Pestilli F, Bullock D, Yeh F-C, Koudoro S, Rokem A, Harezlak J, Garyfallidis E (2020) Bundle analytics, a computational framework for investigating the shapes and profiles of brain pathways across populations. Sci Rep 10:17149

12. Delmaire C, Vidailhet M, Wassermann D, Descoteaux M, Valabregue R, Bourdain F, Lenglet C, Sangla S, Terrier A, Deriche R, Lehericy S (2009) Diffusion abnormalities in the primary sensorimotor pathways in writer's cramp. Arch Neurol 66:502–508

13. Fischl B, Salat DH, Busa E, Albert M, Dieterich M, Haselgrove C, van der Kouwe A, Killiany R, Kennedy D, Klaveness S, Montillo A, Makris N, Rosen B, Dale AM (2002) Whole brain segmentation: automated labeling of neuroanatomical structures in the human brain. Neuron 33:341–355

14. Groth CL, Brown M, Honce JM, Shelton E, Sillau SH, Berman BD (2021) Cervical dystonia is associated with aberrant inhibitory signaling within the thalamus. Front Neurol. https://doi.org/10.3389/fneur.2020.575879

15. Guehl D, Burbaud P, Boraud T, Bioulac B (2000) Bicuculline injections into the rostral and caudal motor thalamus of the monkey induce different types of dystonia. Eur J Neurosci 12:1033–1037

16. Hanssen H, Heldmann M, Prasuhn J, Tronnier V, Rasche D, Diesta CC, Domingo A, Rosales RL, Jamora RD, Klein C, Munte TF, Bruggemann N (2018) Basal ganglia and cerebellar pathology in X-linked dystonia-parkinsonism. Brain 141:2995–3008

17. Jenkinson M, Bannister P, Brady M, Smith S (2002) Improved optimization for the robust and accurate linear registration and motion correction of brain images. Neuroimage 17:825–841

18. Kellner E, Dhital B, Kiselev VG, Reisert M (2016) Gibbs-ringing artifact removal based on local subvoxel-shifts. Magn Reson Med 76:1574–1581

19. Kirke DN, Battistella G, Kumar V, Rubien-Thomas E, Choy M, Rumbach A, Simonyan K (2017) Neural correlates of dystonic tremor: a multimodal study of voice tremor in spasmodic dysphonia. Brain Imag Behav 11:166–175

20. Lampinen B, Szczepankiewicz F, Mårtensson J, van Westen D, Sundgren PC, Nilsson M (2017) Neurite density imaging versus imaging of microscopic anisotropy in diffusion MRI: A model comparison using spherical tensor encoding. Neuroimage 147:517–531

21. LeDoux MS, Lorden JF (2002) Abnormal spontaneous and harmaline-stimulated Purkinje cell activity in the awake genetically dystonic rat. Exp Brain Res 145:457–467

22. Li HQ, Yin B, Quan C, Geng DY, Yu H, Bao YF, Liu J, Li YX (2018) Evaluation of patients with relapsing-remitting multiple sclerosis using tract-based spatial statistics analysis: diffusion kurtosis imaging. BMC Neurol 18:108

23. MacIver CL, Tax CMW, Jones DK, Peall KJ (2022) Structural magnetic resonance imaging in dystonia: A systematic review of methodological approaches and findings. Eur J Neurol 29:3418–3448

24. Miller KL, Alfaro-Almagro F, Bangerter NK, Thomas DL, Yacoub E, Xu J, Bartsch AJ, Jbabdi S, Sotiropoulos SN, Andersson JL, Griffanti L, Douaud G, Okell TW, Weale P, Dragonu I, Garratt S, Hudson S, Collins R, Jenkinson M, Matthews PM, Smith SM (2016) Multimodal population brain imaging in the UK Biobank prospective epidemiological study. Nat Neurosci 19:1523–1536

25. Paydar A (2014) Diffusional kurtosis imaging: a promising technique for detecting microstructural changes in neural development and regeneration. Neural Regen Res 9:1108–1109

26. Pisani A, Martella G, Tscherter A, Bonsi P, Sharma N, Bernardi G, Standaert DG (2006) Altered responses to dopaminergic D2 receptor activation and N-type calcium currents in striatal

cholinergic interneurons in a mouse model of DYT1 dystonia. Neurobiol Dis 24:318–325

27. Pontillo G, Castagna A, Vola EA, Macerollo A, Peluso S, Russo C, Baglio F, Manganelli F, Brunetti A, Cocozza S, Esposito M (2020) The cerebellum in idiopathic cervical dystonia: a specific pattern of structural abnormalities? Parkinsonism Relat Disord 80:152–157

28. Prell T, Peschel T, Kohler B, Bokemeyer MH, Dengler R, Gunther A, Grosskreutz J (2013) Structural brain abnormalities in cervical dystonia. BMC Neurosci 14:123

29. Rittiner JE, Caffall ZF, Hernandez-Martinez R, Sanderson SM, Pearson JL, Tsukayama KK, Liu AY, Xiao C, Tracy S, Shipman MK, Hickey P, Johnson J, Scott B, Stacy M, Saunders-Pullman R, Bressman S, Simonyan K, Sharma N, Ozelius LJ, Cirulli ET, Calakos N (2016) Functional genomic analyses of mendelian and sporadic disease identify impaired eIF2alpha signaling as a generalizable mechanism for dystonia. Neuron 92:1238–1251

30. Rudrapatna U, Parker GD, Roberts J, Jones DK (2021) A comparative study of gradient nonlinearity correction strategies for processing diffusion data obtained with ultra-strong gradient MRI scanners. Magn Reson Med 85:1104–1113

31. Sairanen V, Leemans A, Tax CMW (2018) Fast and accurate Slicewise OutLIer Detection (SOLID) with informed model estimation for diffusion MRI data. Neuroimage 181:331–346

32. Sperandeo A, Tamburini C, Noakes Z, de la Fuente DC, Keefe F, Petter O, Plumbly W, Clifton N, Li M, Peall K (2022) Cortical neuronal hyperexcitability and synaptic changes in SGCE mutation-positive myoclonus dystonia. Brain 146:1523–1541

33. Tseng Y-J, Chen R-S, Hsu W-Y, Hsiao F-J, Lin Y-Y (2014) Reduced motor cortex deactivation in individuals who suffer from Writer's cramp. PLoS ONE 9:e97561

34. Valeriani D, Simonyan K (2020) A microstructural neural network biomarker for dystonia diagnosis identified by a DystoniaNet deep learning platform. Proc Natl Acad Sci 117:26398–26405

35. Veraart J, Novikov DS, Christiaens D, Ades-aron B, Sijbers J, Fieremans E (2016) Denoising of diffusion MRI using random matrix theory. Neuroimage 142:394–406

36. Veraart J, Poot DH, Van Hecke W, Blockx I, Van der Linden A, Verhoye M, Sijbers J (2011) More accurate estimation of diffusion tensor parameters using diffusion Kurtosis imaging. Magn Reson Med 65:138–145

37. Veraart J, Van Hecke W, Sijbers J (2011) Constrained maximum likelihood estimation of the diffusion kurtosis tensor using a Rician noise model. Magn Reson Med 66:678–686

38. Wadon ME, Fenner E, Kendall KM, Bailey GA, Sandor C, Rees E, Peall KJ (2022) Clinical and genotypic analysis in determining dystonia non-motor phenotypic heterogeneity: a UK Biobank study. J Neurol. https://doi.org/10.1007/s00415-022-11307-4

39. Wasserthal J, Maier-Hein KH, Neher PF, Northoff G, Kubera KM, Fritze S, Harneit A, Geiger LS, Tost H, Wolf RC, Hirjak D (2020) Multiparametric mapping of white matter microstructure in catatonia. Neuropsychopharmacology 45:1750–1757

40. Wasserthal J, Neher P, Maier-Hein KH (2018) TractSeg - Fast and accurate white matter tract segmentation. Neuroimage 183:239–253

41. Wasserthal J, Neher PF, Hirjak D, Maier-Hein KH (2019) Combined tract segmentation and orientation mapping for bundle-specific tractography. Med Image Anal 58:101559

42. Wasserthal J, Neher PF, Maier-Hein KH (2018) Tract Orientation Mapping for Bundle-Specific Tractography. In: Frangi AF, Schnabel JA, Davatzikos C, Alberola-López C, Fichtinger G (eds) Medical Image Computing and Computer Assisted Intervention – MICCAI 2018. Springer International Publishing, Cham, pp 36–44

43. Xing H, Yokoi F, Walker AL, Torres-Medina R, Liu Y, Li Y (2022) Electrophysiological characterization of the striatal cholinergic interneurons in Dyt1 ΔGAG knock-in mice. Dystonia. https://doi.org/10.3389/dyst.2022.10557

44. Zhang H, Schneider T, Wheeler-Kingshott CA, Alexander DC (2012) NODDI: practical in vivo neurite orientation dispersion and density imaging of the human brain. Neuroimage 61:1000–1016

45. Zito GA, Tarrano C, Ouarab S, Jegatheesan P, Ekmen A, Béranger B, Valabregue R, Hubsch C, Sangla S, Bonnet C, Delorme C, Méneret A, Degos B, Bouquet F, Apoil Brissard M, Vidailhet M, Hasboun D, Worbe Y, Roze E, Gallea C (2023) Fixel-based analysis reveals whole-brain white matter abnormalities in cervical dystonia. Movem Disord. https://doi.org/10.1002/mds.29425